Intracavity frequency-doubled femtosecond Cr^{4+}:forsterite laser

Tzu-Ming Liu, Shi-Peng Tai, and Chi-Kuang Sun

The generation of femtosecond optical pulses centered at ~620 nm directly from an all-solid-state laser oscillator is reported. Red pulses with pulse widths of the order of 170 fs were obtained with 24-mW average power at an 81-MHz repetition rate. They were achieved by intracavity frequency doubling of a mode-locked Cr^{4+}:forsterite laser with a 1-mm-thick β-BaB_2O_4 crystal. The process of laser mode locking was modified by surface coating the doubling crystal. © 2001 Optical Society of America

OCIS codes: 140.3070, 140.4050, 140.5680, 190.2620, 320.2250.

1. Introduction

Colliding-pulse mode-locked dye lasers centered at 600–620 nm were once the unique source of short femtosecond optical pulses.[1–3] Following recent advances in mode-locking techniques in all-solid-state lasers, the compactness, high output power, and newly developed mode-locking mechanisms [e.g., Kerr-lens mode locking (KLM)] of solid-state lasers make them attractive replacements for femtosecond dye-laser sources. However, there is no broadband all-solid-state laser crystal operating near 600–620 nm whose dye-laser counterpart has already been widely applied for scientific studies.

To obtain the advantage of femtosecond all-solid-state lasers and at the same time maintain the unique wavelengths occupied by the colliding-pulse mode-locked dye lasers, frequency doubling from a Cr^{4+}:forsterite laser operating between 1.17 and 1.34 μm is the most obvious choice. Sennaroglu *et al*. reported the use of external-cavity frequency doubling of a Cr^{4+}:forsterite laser with a 2-mm-thick $LiIO_3$ crystal to obtain 116-fs (FWHM) pulses at 615 nm.[4] Similar external-cavity frequency doubling was reported from a cavity-dumped KLM Cr^{4+}:forsterite laser with a 0.7-mm-thick β-BaB_2O_4 (BBO) crystal to achieve 49-fs pulses.[5] To increase the external doubling efficiency, a resonant cavity containing a thin BBO crystal was used, and 116-fs red pulses were reported.[6] Based on considerations of configuration simplicity and conversion efficiency, intracavity frequency doubling is a better choice than external-cavity frequency doubling, especially for laser cavities with long optical pulses and low output powers. Relatively high intracavity optical power can provide more-efficient conversion and produce stronger doubled output. The use of intracavity doubling can also prevent the complication of prism dispersion compensation of the fundamental output before external doubling. Backus *et al*. demonstrated intracavity frequency doubling in a Ti:sapphire laser, and femtosecond pulses were generated at 416 nm directly from the laser oscillator.[7] For a Cr^{4+}:forsterite laser, Qian *et al*. placed a LiB_3O_5 crystal into a laser cavity to help in KLM and to generate fundamental pulses as short as 60 fs.[8] These early studies showed that the mode-locking condition can be satisfied after insertion of a doubling crystal in a Cr^{4+}:forsterite laser. However, an early attempt at intracavity frequency doubling of a femtosecond Cr:forsterite laser reported by Yanovsky and Wise[6] indicated less-stable laser operation.

In our research we used a 1-mm-thick BBO crystal to generate 170-fs red pulses, centered about 620 nm, directly from an all-solid-state laser oscillator by using intracavity frequency doubling of a femtosecond mode-locked Cr^{4+}:forsterite laser. Stable laser operation was achieved with the help of a semiconductor saturable-absorber mirror (SESAM).

2. Experimental Setup

Figure 1 is a diagrammatic representation of the laser resonator setup. The laser constructed for this study uses a 19-mm-long Brewster-cut Cr^{4+}:forsterite crystal with its *b* axis on the horizontal plane, resulting in horizontal polarization for the lasing fundamental

The authors are with the Department of Electrical Engineering and Graduate Institute of Electro-Optical Engineering, National Taiwan University, Taipei 10617, Taiwan. The e-mail address for C.-K. Sun is sun@cc.ee.ntu.edu.tw.

Received 9 June 2000; revised manuscript received 3 January 2001.
0003-6935/01/121957-04$15.00/0

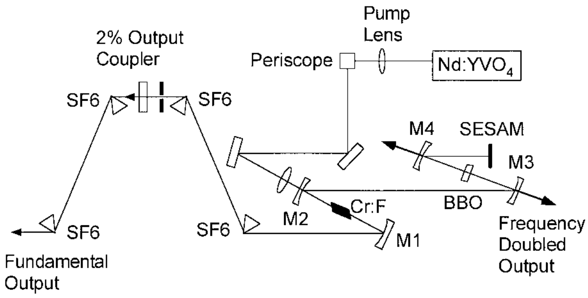

Fig. 1. Schematic diagram of the intracavity frequency-doubled femtosecond Cr^{4+}:forsterite laser.

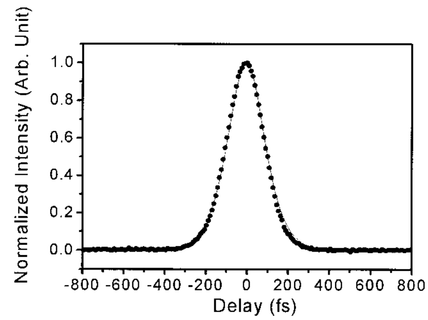

Fig. 2. Autocorrelation trace (filled circles) and its $sech^2$ fit (solid curve) of the Cr^{4+}:forsterite laser output without the doubling crystal at 1230 nm. The FWHM of the autocorrelation trace is 215 fs.

beam. The crystal temperature was kept near 2 °C. The laser was pumped with 8 W of 1064-nm light from a diode-pumped $Nd:YVO_4$ laser (Spectra-Physics Millennia IR). At the output of the pump laser, a pump lens was placed such that the size of the pumping laser beam could be adjusted. After the pump beam's polarization was rotated by a periscope, it was focused with a 10-cm lens through highly reflecting cavity mirror M2 onto the Cr^{4+}:forsterite crystal. The laser cavity was a modified Z cavity that consisted of a 2% output coupler, four laser mirrors (M1–M4), and a SESAM. For intracavity frequency doubling, the lack of a self-starting mechanism for KLM makes cavity alignment difficult. Use of the SESAM initiates and stabilizes the femtosecond pulse generation. This technique has been applied to mode lock Cr^{4+}:forsterite lasers,[9,10] and optical pulses as short as 36 fs were obtained.[11] In our study the SESAM consisted of 25 periods of GaAs/AlAs quarter-wave layers followed by an $Al_{0.48}In_{0.52}As$ quarter-wave layer with two embedded $Ga_{0.47}In_{0.53}As$ quantum wells. To provide the saturable-absorber nonlinearity for initiating and stabilizing the Cr^{4+}:forsterite laser, we designed the quantum-well structure to have heavy-hole excitonic resonance at 1232 nm at room temperature. The insertion loss of the SESAM was 2.5%, with a saturation energy of ~50 $\mu J/cm^2$. M1–M4 were mirrors with 10-cm radii of curvature that were highly reflection coated (>99%) for the spectral range of the fundamental output (1200–1270 nm). M1, M2, and M4 had 50% transmission near 620 nm, whereas M3 was designed to have 75% transmission near 620 nm. All the mirrors formed three beam waists in the cavity, and their nominal calculated mode sizes were of the order of 10^{-4} cm^2. The Cr^{4+}:forsterite crystal was placed between M1 and M2, and the crystal between M3 and M4 was a nonlinear crystal for intracavity frequency doubling. The last beam waist lay on the SESAM through mirror M4 at one end of the cavity. On the other side of the cavity, an SF6 prism pair was inserted with 30-cm separation to provide intracavity group-velocity dispersion compensation. We used a slit before the output coupler to tune the fundamental wavelength. Outside the cavity we used another SF6 prism pair with the same 30-cm separation for both beam shaping and dispersion compensation of the fundamental output. Three BBO crystals, with thicknesses of 1, 0.3, and 0.1 mm, were prepared for the intracavity frequency-doubling experiment. All were double-side antireflection coated for the fundamental wavelength and for the frequency-doubled wavelength. Using the dispersion relation in BBO crystal from Ref. 12 with

$$n_0^2 = A + B/(\lambda^2 - C) - D\lambda^2, \qquad (1)$$

$$n_e^2 = E + F/(\lambda^2 - G) - H\lambda^2, \qquad (2)$$

where $A = 2.7359$, $B = 0.01878$, $C = 0.01822$, $D = 0.01354$, $E = 2.3753$, $F = 0.01224$, $G = 0.01667$, and $H = 0.01516$.[12] We calculated a phase-matching bandwidth of the 1-mm-thick BBO at 1240 nm to be ~56 nm, which is sufficient to support the bandwidth required for femtosecond second-harmonic generation.

3. Intracavity Frequency Doubling with BBO

Without insertion of the BBO crystal, 110-mW stable fundamental output power can be obtained at 1230 nm. Its corresponding autocorrelation trace is shown in Fig. 2 with 215-fs FWHM, indicating a 140-fs pulse width when a $sech^2$ profile is assumed. The pulse width obtained was limited by the narrow reflection bandwidth and the high positive third-order dispersion of our SESAM.[10] We can tune the central wavelength of the output pulse by adjusting the lateral position of the slit behind the prism pairs. Figure 3 shows the corresponding spectrum from the Cr^{4+}:forsterite laser centered at 1230 nm. The central output wavelength can be tuned from ~1220 to ~1240 nm, limited by the SESAM resonance wavelength, with 20-nm bandwidth during operation at 1230 nm. By removing the SESAM from the laser cavity we could extend the tuning range of the mode-locked laser to 1270 nm by using a KLM mechanism, where the tunability was limited by the high-reflection coatings of the cavity mirrors and the output coupler.

After placing the 1-mm-thick BBO crystal with type I phase matching at the beam waist between M3 and M4, we obtained stable generation of 24-mW (14 mW from M3 and 10 mW from M4) frequency-doubled red output while the corresponding fundamental output power dropped to 95 mW. The repetition rate was 81 MHz, which was synchronized with the fundamental

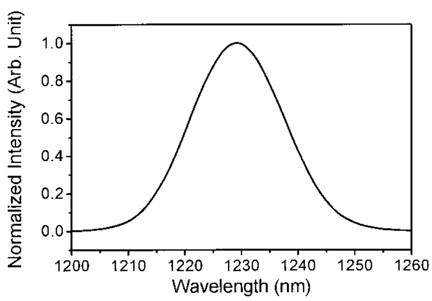

Fig. 3. Spectrum of the Cr^{4+}:forsterite laser output without the doubling crystal.

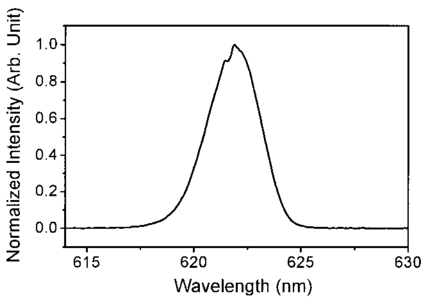

Fig. 4. Red output spectrum of the intracavity frequency-doubled femtosecond Cr^{4+}:forsterite laser.

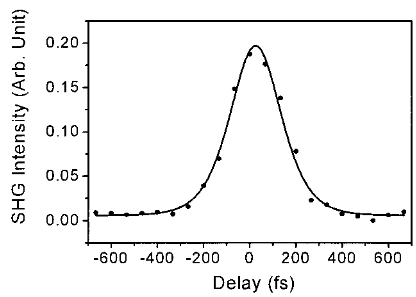

Fig. 5. Autocorrelation trace of the intracavity frequency-doubled Cr^{4+}:forsterite laser (filled circles) and its sech^2 fit (solid curve). The FWHM autocorrelation pulse width is 240 fs, corresponding to a pulse width of 168 fs. SHG, second-harmonic generation.

pulse train. To compare the net conversion efficiency with external-cavity frequency doubling, we also performed external-cavity frequency doubling on the same 1-mm-thick BBO crystal, using a 5-cm focal-length objective with the 110-mW fundamental output without the BBO crystal inside the laser cavity. Only 240 μW of optimized red light could be obtained, indicating a 100-fold power increase with the intracavity frequency-doubling scheme, primarily as a result of the much higher optical power inside the laser cavity. Figure 4 shows the spectrum of the frequency-doubled output with a bandwidth of 2.9 nm centered at 622 nm. Its corresponding autocorrelation trace is shown in Fig. 5. By fitting the data with a sech^2 intensity profile we obtained 260-fs FWHM, which corresponds to 168-fs pulse FWHM. The time–bandwidth product was 0.378, which is 1.2 times the transform limit (0.315) of a sech^2 pulse.

When the angle of the BBO was moved slightly off the horizontal axis, the red output was found to be tunable from 617 nm [with a bandwidth of 4.1 nm; solid curve in Fig. 6(a)] to 624 nm [with a bandwidth of 3.5 nm; dotted curve of Fig. 6(a)]. Even though turning the BBO about a horizontal axis corresponds to tuning the phase-matching wavelength, the frequency tuning of the red output should not originate from the variation of phase-matching wavelength owing to a much wider phase-matching bandwidth. We measured the fundamental output spectra for several tuning angles. Figure 6(b) shows the corresponding fundamental spectra of the 617- and 624-nm red output. Shifted center frequencies of 1234 and 1248 nm with bandwidths of 11 and 7.4 nm, respectively, could be observed when we altered the BBO crystal angle. The observed wavelength shifting of the fundamental spectra with the frequency-doubled output ruled out the possibility that this wavelength tuning was influenced by the shift of the maximum phasing-matching wavelength with different crystal angles. If the tuning is due to the change of BBO's phase-matching wavelength at different angles, the fundamental wavelength should not change as the BBO angle is varied. Similar behavior can also be observed with the 0.3- and 0.1-mm-thick BBO crystals, with even wider phase-matching bandwidths and phase-matching angles, which further ruled out the influence of different phase-matching conditions. The rest of the mechanism for frequency tuning should then be the surface coating effect related to the fundamental wavelength.

One possible wavelength-tuning mechanism is the shifted reflection minimum wavelength of the surface antireflection coating for the fundamental wavelength as we altered the BBO crystal angle. To confirm this assumption we measured the reflection spectrum of the BBO surface coating. For the measurement we employed a quartz tungsten halogen lamp as the broadband light source and used a monochromator to select the incident wavelength with a slit. The light source that diverged from the slit was collimated and

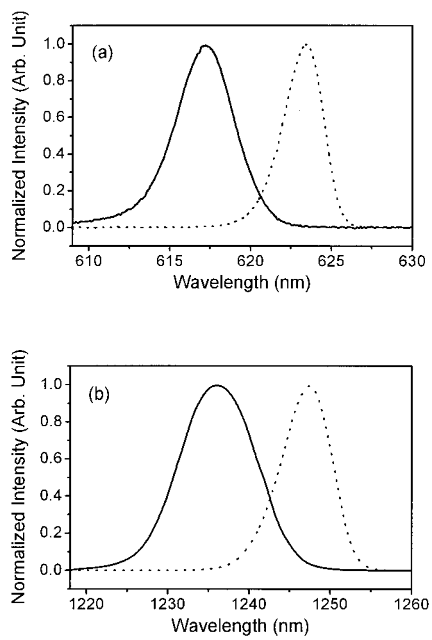

Fig. 6. Output spectra of the intracavity-doubled femtosecond Cr^{4+}:forsterite laser for (a) frequency-doubled light and (b) the corresponding fundamental light with different BBO crystal angles.

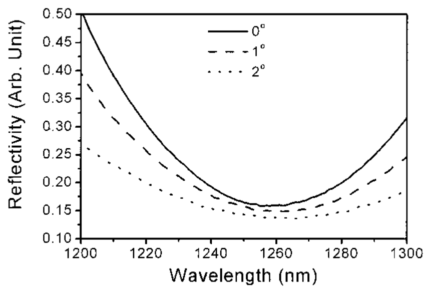

Fig. 7. Reflection spectra of the BBO crystal at three incidence angles: 0°, 1°, and 2°. Their reflection minima reside at 1256, 1262, and 1267 nm, respectively.

horizontally polarized with a polarizer to reconstruct the same conditions as in the laser cavity. By using a beam splitter we directed the monochromatic light to a lens with a 15-cm focal length and focused it onto the BBO crystal, which was placed suitably for type I phase matching. The reflected light was collected by the same lens, passed through the beam splitter, and then focused onto an IR detector (Newport 818-IR). We chopped the input light and recorded the reflection light's intensity as a function of wavelength, using a lock-in amplifier. Figure 7 shows the measured reflection spectra that correspond to crystal angles (or incident angles) of 0°, 1°, and 2°. A reflection minimum shift from 1256 to 1267 nm could be observed when the crystal angle was altered from 0° to 2°. This minimum reflection wavelength shift shares the same trend as the laser fundamental wavelength shift, supporting the assumption that the surface antireflection coating should be one of the mechanisms that are responsible for wavelength tuning. This redshifted coating wavelength, compared with the SESAM resonance wavelength, should also be responsible for redshifting the fundamental output wavelength after insertion of the BBO crystal. The measured narrow transmission bandwidth of the BBO surface coating for the fundamental wavelength could also be responsible for the reduction of the fundamental bandwidth by one half after insertion of the doubling crystal. With an improved broadband surface coating, higher red output power with shorter pulses could be expected. We could also achieve higher conversion efficiency by shortening the pulse width with an improved SESAM reflection bandwidth or by use of a thicker BBO crystal with a narrower phase-matching bandwidth. Moreover, high conversion efficiency has been reported for external-cavity frequency doubling with lithium triborate (Ref. 13) and for Type II phase-matching $KTiOPO_4$,[14] indicating that better performance could be achieved when these crystals are used for intracavity frequency doubling.

4. Summary

In summary, we have demonstrated the generation of femtosecond optical pulses centered at ~620 nm directly from an all-solid-state laser oscillator. Pulses of the order of 170 fs with 24-mW average power at an 81-MHz repetition rate were obtained by intracavity frequency doubling of a mode-locked Cr^{4+}:forsterite laser with a 1-mm-thick β-BaB_2O_4 crystal. Stable laser operation was achieved with the help of a SESAM. We were able to tune the output wavelength by changing the BBO crystal angle. This tuning mechanism is attributed partly to angle-dependent surface coating of the doubling crystal.

The authors acknowledge the technical support of Jiun-Chien Wang, Chih-Ming Lai, Gwo-Jen Jan, Ying-Jay Yang, and Anatoly Ivanov. This study is sponsored by the National Science Council of Taiwan under grant NSC 89-2215-E-002-064.

References

1. R. L. Fork, B. I. Greene, and C. V. Shank, "Generation of optical pulses shorter than 0.1 psec by colliding pulse mode locking," Appl. Phys. Lett. **38,** 671–672 (1981).
2. W. H. Knox, R. L. Fork, M. C. Downer, R. H. Stolen, C. V. Shank, and J. A. Valdmanis, "Optical pulse compression to 8 fs at a 5-kHz repetition rate," Appl. Phys. Lett. **46,** 1120–1121 (1985).
3. R. L. Fork, C. H. Brito Cruz, P. C. Becker, and C. V. Shank, "Compression of optical pulses to six femtoseconds by using cubic phase compensation," Opt. Lett. **12,** 483–485 (1987).
4. A. Sennaroglu, C. R. Pollock, and H. Nathel, "Generation of tunable femtosecond pulses in the 1.21–1.27 μm and 605–635 nm wavelength region by using a regeneratively initiated self-mode-locked Cr:forsterite laser," IEEE J. Quantum Electron. **30,** 1851–1861 (1994).
5. E. Slobodchikov, J. Ma, V. Kamalov, K. Tominaga, and K. Yoshihara, "Cavity-dumped femtosecond Kerr-lens mode locking in a chromium-doped forsterite laser," Opt. Lett. **21,** 354–356 (1996).
6. V. P. Yanovsky and F. W. Wise, "Frequency doubling of 100-fs pulses with 50% efficiency by use of a resonant enhancement cavity," Opt. Lett. **19,** 1952–1954 (1994).
7. S. Backus, M. T. Asaki, C. Shi, H. C. Kapteyn, and M. M. Murnane, "Intracavity frequency doubling in a Ti:sapphire laser: generation of 14-fs pulses at 416 nm," Opt. Lett. **19,** 399–401 (1994).
8. L. J. Qian, X. Liu, and F. W. Wise, "Femtosecond Kerr-lens mode locking with negative nonlinear phase shifts," Opt. Lett. **24,** 166–168 (1999).
9. P. T. Guerreiro, S. Ten, E. Slobochikov, Y. M. Kim, J. C. Woo, and N. Peyghambarian, "Self-starting mode-locked Cr:forsterite laser with semiconductor saturable Bragg reflector," Opt. Commun. **136,** 27–30 (1997).
10. Z. Zhang, K. Torizuka, T. Itatani, K. Kobayashi, T. Sugaya, and T. Nakagawa, "Self-starting mode-locked femtosecond forsterite laser with a semiconductor saturable-absorber mirror," Opt. Lett. **22,** 1006–1008 (1997).
11. Z. Zhang, K. Torizuka, T. Itatani, K. Kobayashi, T. Sugaya, and T. Nakagawa, "Femtosecond Cr:forsterite laser with mode locking initiated by a quantum-well saturable absorber," IEEE J. Quantum Electron. **33,** 1975–1981 (1997).
12. V. G. Dmitriev, G. G. Gurzadyan, and D. N. Nikogosyan, "Properties of nonlinear optical crystals" in *Handbook of Nonlinear Optical Crystals*, 2nd ed., V. G. Dmitriev, G. G. Gurzadyan, and D. N. Nikogosyan, eds. (Springer-Verlag, Berlin, 1997), Chap. 3.1.5, pp. 96–103.
13. X. Liu, L. Qian, and F. W. Wise, "Efficient generation of 50-fs red pulses by frequency doubling in LiB_3O_5," Opt. Commun. **144,** 265–268 (1997).
14. J. C. Diettrich, I. T. McKinnie, and D. M. Warrington, "Tunable high-repetition-rate visible solid-state lasers based on intracavity frequency doubling of Cr:forsterite," IEEE J. Quantum Electron. **35,** 1718–1723 (1999).